

Supporting Information

Direct deposition of dense YSZ/Ni-YSZ thin-film bilayers on porous anode-supported cells with high performance and stability

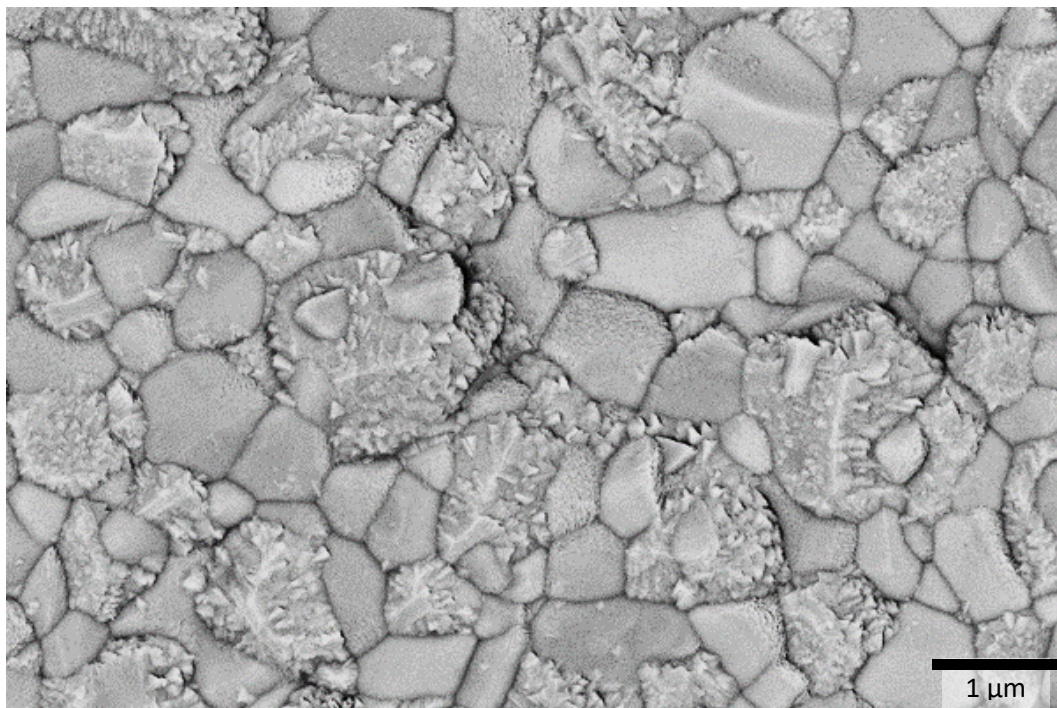
Katherine Develos-Bagarinao,^{*a} Toshiaki Yamaguchi^b and Haruo Kishimoto^a

^aGlobal Zero Emission Research Center, National Institute of Advanced Industrial Science and Technology, AIST West, 16-1 Onogawa, Tsukuba, Ibaraki 305-8569, Japan

^bEnergy Process Research Institute, National Institute of Advanced Industrial Science and Technology, AIST Tsukuba West, 16-1 Onogawa, Tsukuba, Ibaraki, 305-8569, Japan

* Corresponding author. Email: develos-bagarinao@aist.go.jp

(a)



(b)

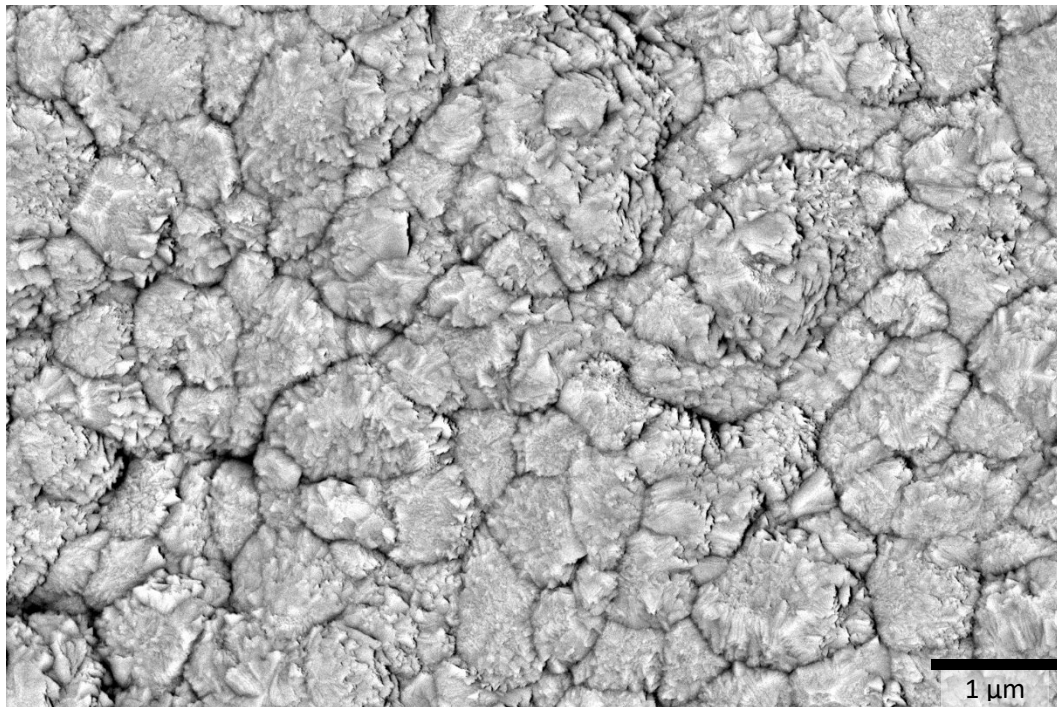
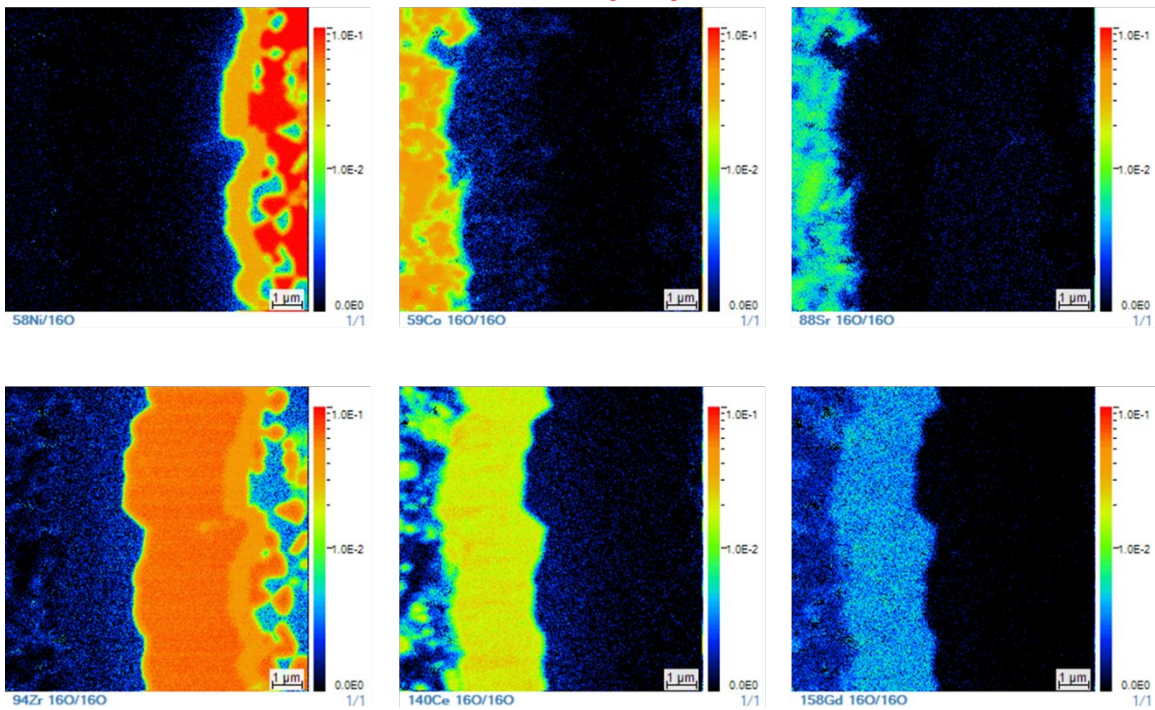


Figure S1. Typical plan-view SEM images depicting the YSZ thin film surface morphologies deposited on AFL/anode-supported cells a) without and b) with NiO-YSZ nanocomposite layer. Without the NiO-YSZ nanocomposite layer, YSZ grains exhibit a bimodal grain distribution, i.e., less homogeneous layer.

PLD-YSZ, as-prepared



PLD-YSZ, tested

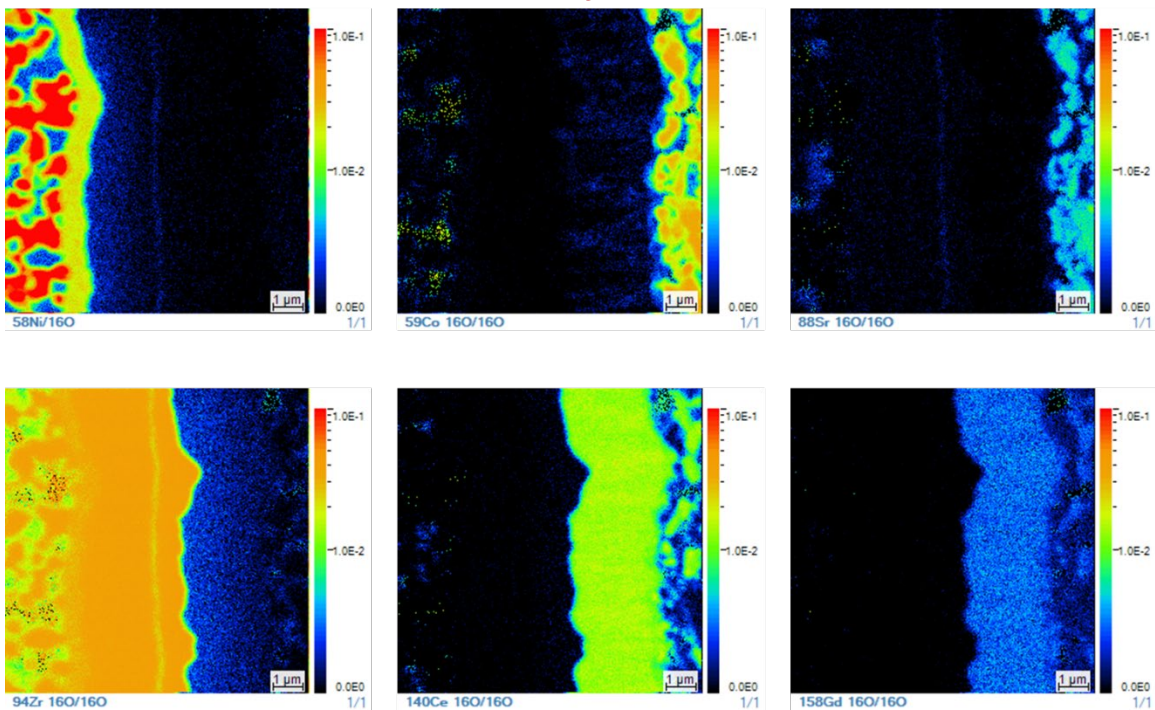
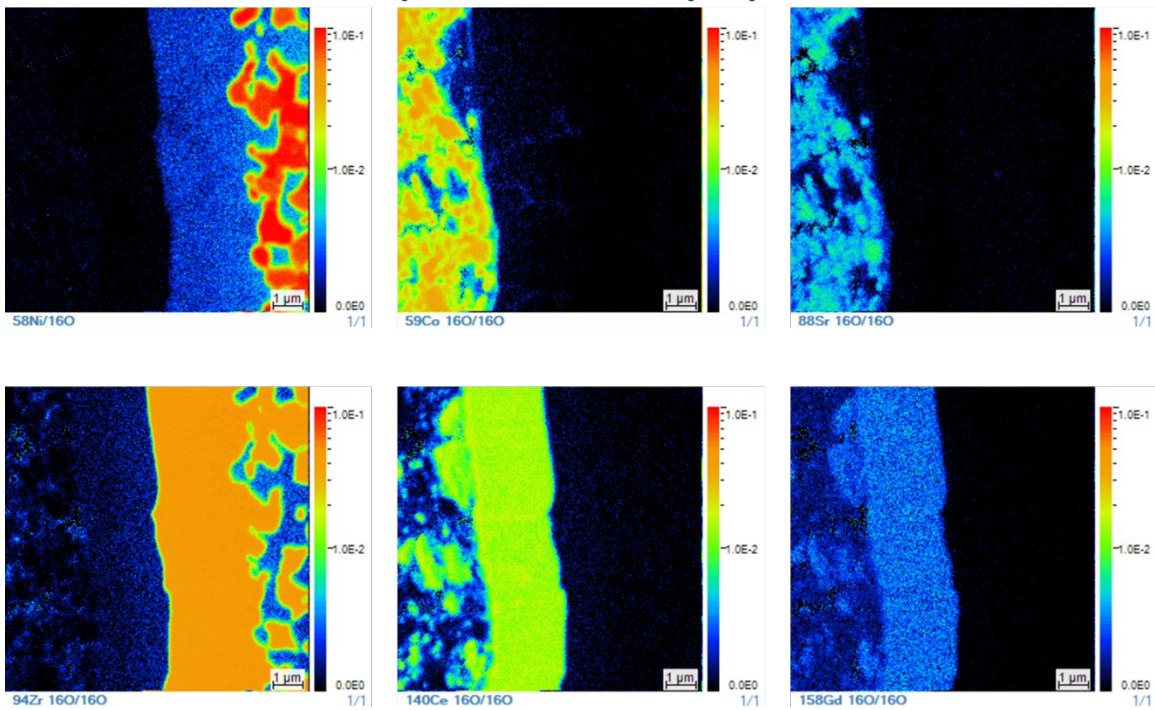


Figure S2. SIMS elemental mapping of ^{58}Ni , $^{59}\text{Co}^{16}\text{O}^-$, $^{88}\text{Sr}^{16}\text{O}^-$, $^{94}\text{Zr}^{16}\text{O}^-$ and $^{140}\text{Ce}^{16}\text{O}^-$ normalized by $^{16}\text{O}^-$ for PLD-5 (PLD-YSZ layer).

Screen-printed YSZ, as-prepared



Screen-printed YSZ, tested

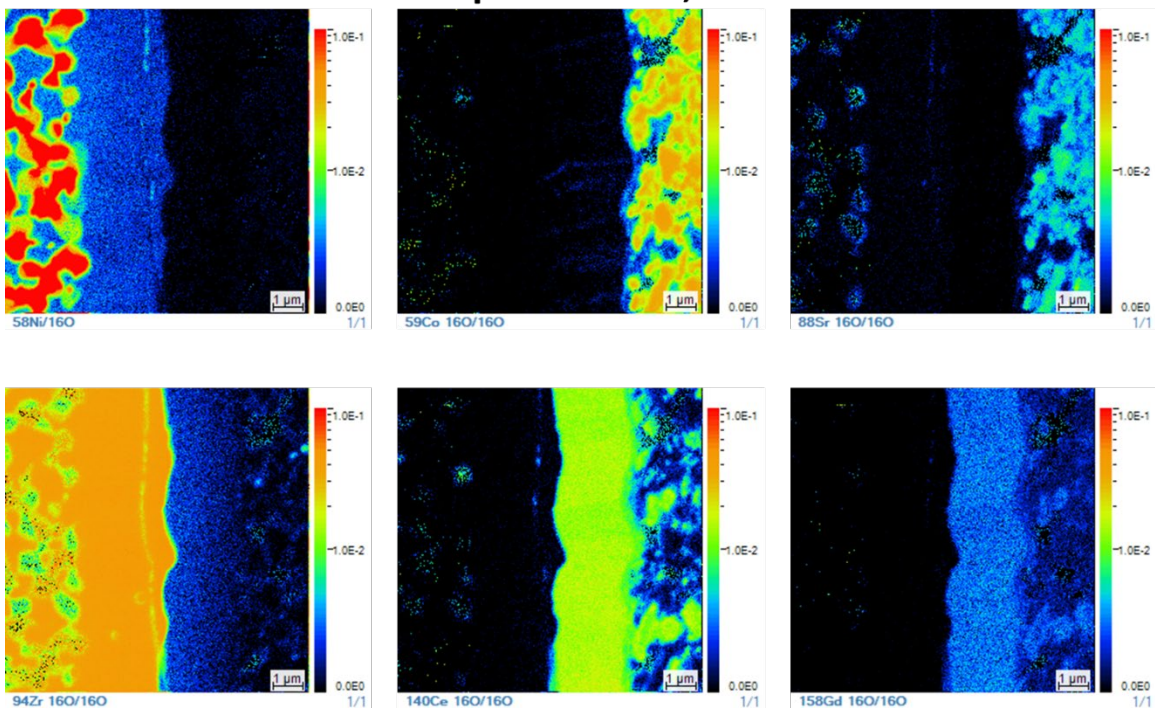


Figure S3. SIMS elemental mapping of $^{58}\text{Ni}^-$, $^{59}\text{Co}^{16}\text{O}^-$, $^{88}\text{Sr}^{16}\text{O}^-$, $^{94}\text{Zr}^{16}\text{O}^-$ and $^{140}\text{Ce}^{16}\text{O}^-$ normalized by $^{16}\text{O}^-$ for SP-2 (screen-printed YSZ layer).